Hindawi
Geofluids
Volume 2022, Article ID 7135465, 15 pages
https://doi.org/10.1155/2022/7135465

Research Article

Optimization Analysis of Pretreatment Device Structural Parameters for Low-Concentration CBM Utilization

Lu Xiao [1,2,3]

[1]*China Coal Technology Engineering Group Chongqing Research Institute, Chongqing 400037, China*
[2]*National key Laboratory of Gas Disaster Detecting Preventing and Emergency Controlling, Chongqing 400037, China*
[3]*Research Center of Fluid Machinery Engineering and Technology, Jiangsu University, Zhenjiang 212013, China*

Correspondence should be addressed to Lu Xiao; xiaolu8317@126.com

Received 7 June 2022; Revised 31 July 2022; Accepted 8 August 2022; Published 22 August 2022

Academic Editor: Quanle Zou

The unstable concentration of the difficulty in utilizing low-concentration CBM causes a large amount of CBM to be discharged into the atmosphere. In order to ensure the safe and stable operation of the CBM utilization device, the gas mixing unit is used to stabilize the concentration of feed gas. Generally, the resistance of the gas mixing unit is not higher than 500 Pa and the uniformity of gas is not less than 90%. In order to solve the problems of heavy resistance and low uniformity of the existing CBM mixing unit, a three-dimensional calculation model is established, and the structural parameters such as the number of spiral blades, blade length, and pitch in the gas mixing unit are adjusted and verified by experiments to achieve optimal performance. The dimensionless mathematical correlation between the resistance loss and the uniformity of gas is refined, and the maximum error between the resistance loss and the simulation results is controlled within 10%; it provides a theoretical basis for the uniformity and low resistance mixing of different gases in the gas industry. When the flow is 7000 Nm^3/h, 50000 Nm^3/h, and 160000 Nm^3/h, respectively, the optimal structural parameters of the mixing zone are as follows: the number of blades is 3, 3, and 2, respectively, the pitch is 1000 mm, 2000 mm, and 2636 mm, respectively, and the length of blades is 500 mm, 1600 mm, and 1845 mm, respectively. The optimal structural parameters of the small pipe area are as follows: the mixing device with a flow of 50000 Nm^3/h is not equipped with blades, the number of blades of the other two devices is 4, the pitch is 1400 mm, and the length of blades is 700 mm.

1. Introduction

Coalbed methane (CBM) is homologous with coal, and its main component is methane [1]. Methane is the second largest greenhouse gas after carbon dioxide [2], and its warming effect and potential are higher than carbon dioxide, which has a significant impact on the global greenhouse effect [3]. In recent years, methane emission reduction has become the focus of many areas of research [4]. To eliminate the phenomenon of "no exploring CBM or exploring CBM without producing," the policy of "producing gas first, producing coal second" must be implemented [5, 6]. In addition to producing coal mines, a large amount of CBM is released during coal mining [7–9]. Anthropogenic methane emissions on earth are mainly produced from the process of coal mining and agricultural production [10]. The methane leakage in the global oil and gas industry is 80 million tons, of which the methane emission from coal mines is 40 million tons in 2018. As a clean energy [11–13], CBM has a low utilization rate, and a large amount of CBM is discharged into the atmosphere, resulting in environmental pollution [14, 15].

In 2021, the United States and China reached the *China-US Joint Statement on Climate Crisis* [16] and the *Glasgow Joint Declaration of the United States and China on Intensified Climate Action in the 2020s*. It proposes to formulate a methane emission reduction action plan and control non-carbon dioxide greenhouse gases [17], which is the "first move" for China and the United States to lead global climate governance. As the impact of methane on climate is 25 times

that of carbon dioxide [18], coalbed methane has a huge potential for carbon reduction in the mining process [19], so the utilization of CBM should be an area of focus.

Low-concentration CBM has low calorific value and pressure is uneconomical to reuse after long-distance transportation and can only be used locally in coal mining areas [20]. The low-concentration CBM with a concentration of 10% to 30% is generally used for power generation. However, the generator requires that the methane concentration in the CBM should not change more than 2% within 30 seconds. If the concentration change exceeds this range, the generator will automatically shut down. Low-concentration CBM with a concentration below 10% generally provides heat to users by means of heat storage and oxidation [21]. However, excessively low concentration will result in insufficient heat generated by the unit to maintain the heat balance of its own operation and ultimately lead to furnace blowout, and excessively high concentration may cause explosions [22]. Therefore, in order to ensure the safe and stable operation of CBM thermal storage oxidation unit and coalbed methane power generation unit, it is necessary to adopt a gas mixing unit to stabilize the concentration of raw gas [23].

CBM is mainly extracted from a fractured coal seam by a water ring vacuum pump [24], and the pressure is generally only about 5000 Pa. If the air mixing device resistance is too large, it is impossible to ensure the continuous and stable operation of the rear end utilization unit. Regenerative oxidation unit for feed gas of methane in the cross section of average concentration is around 1.2% [25]. Since the diameter of the inlet pipe is generally not less than 1 meter, if the uniformity of the gas mixing device is not enough, it is very likely that the concentration of methane in some areas of the cross-section of the pipe will be greater than 5% (the lower explosion limit of methane), resulting in the explosion of the thermal storage oxidation device. According to experience, it is generally required that the resistance of CBM gas mixing unit is not more than 500 Pa and the uniformity is not less than 90%.

Aiming at the problems of low gas mixing uniformity and large resistance of CBM mixing unit, this paper studies the construction method of three-dimensional calculation model of internal flow and gas mixing process of CBM mixing unit, reveals the influence of spiral structure parameters on the uniformity and resistance loss, optimizes the number, length, and pitch of spiral blades in the device, and carries out experimental verification. The dimensionless mathematical correlation between resistance loss and the uniformity is refined, which provides a theoretical basis for the uniformity and low resistance mixing of different gases in the gas industry.

2. Model Construction

2.1. Geometric Model. In the process of numerical simulation of the low-concentration CBM gas mixing unit, UG software was used for 3D modeling, HYPERMESH software was used for mesh division, and ANSYS was used for material calculation. Figure 1 shows the geometry of the 7000 Nm^3/h gas mixing unit. For convenience, the outlet of high-concentration methane pipeline to the outlet of the gas mixing unit is defined as the mixing zone, the inside of the high-concentration methane pipeline is defined as the tubule zone, and the flange inlet of the unit to the outlet of the high-concentration methane pipeline is defined as the large pipe zone, as shown in Figure 2. The inner blade of air mixing unit uses a spiral structure with thickness of 6 mm. The gas in the large pipe area and the small pipe area is separated by the pipe wall of the small pipe area. Before entering the mixing area, the two gases do not contact. After entering the mixing area, they begin to contact and mix. The small pipe extends radially into the center of the large pipe area from the hole on the pipe wall of the large pipe, and a 90° elbow is used to change the direction from radial to axial, and spiral blades are set from the end of the elbow.

The CBM at the two inlets in Figure 1 comes from two different gas extraction pump stations. During the actual operation, the concentration will often change, but the CBM utilization device requires that the concentration at the outlet of the gas mixing device be stable. The measure to ensure the stability of the concentration is to adjust the opening of the regulating valves installed on the two inlet pipelines according to the change of the outlet concentration through the pre-set program of the PLC system.

At the beginning of the simulation, gas outlet is set at the cut-off position of the end of the mixing unit. Through calculation, it is found that there is an obvious backflow at the outlet of the unit, which affects the convergence of the calculation results [26]. The main reason lies in that the vortex generated by the flow in the gas mixing unit is not completely in the calculation domain at the outlet, which affects the free flow of gas in the flow field. The front end of the vortex outlet is a shrinking body, and the downstream is connected to a straight cylindrical pipe. The streamline of the fluid will change at this outlet. If the calculation is stopped suddenly, the convergence of FLUENT calculation may be affected, resulting in inaccurate calculation results. Therefore, the outlet extension of 6 m and the inlet extension of 1 m are set in all computational domain models in this paper. In addition, considering that the existence of the nut hole in the actual model affects the mesh quality, in the geometric model adopted in this time, the spiral blades and the pipe wall are set as a seamless connection, and the blades are connected with each other through a solid shaft. A tetrahedral mesh generation method is adopted in the gas mixing device, with a size of 20 mm and a total mesh of about 1.2 million. Since the blades of the unit are in the high-speed gas collision region, the mesh of local blades is encrypted to improve the calculation accuracy.

2.2. Mathematical Model. In the process of solving, the SIMPLIE algorithm is used to solve the governing equation, and the second-order upwind difference scheme is used to realize discreteness [27]. The convergence accuracy is 10^{-6}. When the monitoring results remain constant after 5000 iterations, the calculated results are considered to have converged. The numerical simulation of gas mixing unit is essential to solve

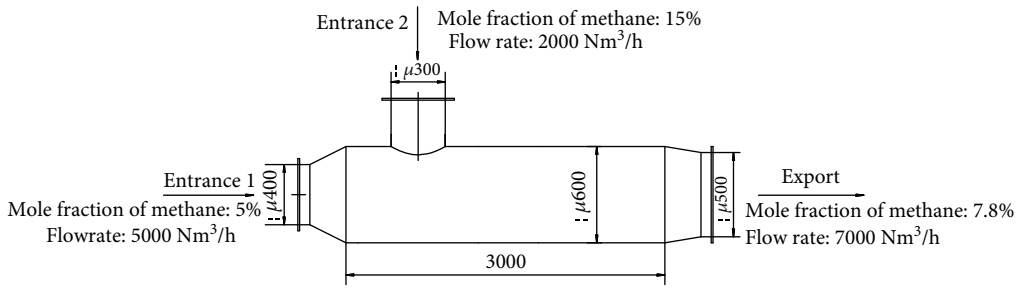

Figure 1: Geometry of the 7000 Nm^3/h gas mixing unit.

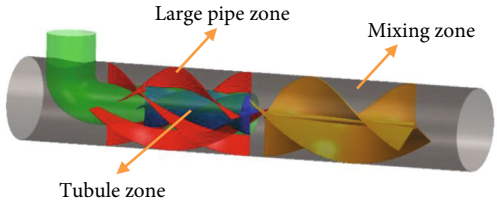

Figure 2: Naming of mixing unit area.

the continuity equation, momentum equation, energy equation and component transport equation, and its expression is as follows:

Continuity equation:

$$\frac{\partial}{\partial x_i}(\rho u_i) = 0, \tag{1}$$

where ρ is the density of the mixture, u_i is the velocity component in i direction, and x_i is the coordinate component in each direction.

The following is the momentum conservation equation:

$$\frac{\partial}{\partial x_j}\left(\rho u_i u_j - \tau_{ij}\right) = -\frac{\partial p}{\partial x_i}, \tag{2}$$

where p is the pressure and τ_{ij} is the pressure tensor.

The following is the energy conservation equation:

$$\frac{\partial}{\partial x_j}\left(\rho u_j h + F_{h,j}\right) = u_j \frac{\partial P}{x_j} + \tau_{ij}\frac{\partial u_i}{\partial x_j}, \tag{3}$$

where h is the static total enthalpy and $F_{h,j}$ is the energy flux in the x_j direction.

The following is the component transport equation:

$$\frac{\partial}{\partial x_j}\left(\rho u_j m_l + J_{l,j}\right) = R_l. \tag{4}$$

In the component transport equation, m_l is the mass fraction of component l, $J_{l,j}$ is the diffusion flux of component l in the x_j direction, and R_l is the formation rate of chemical reaction of component l.

The resistance of the gas mixing unit ΔP is determined by calculation and compared with the experimental measured value to verify the accuracy of the calculation. The experimental measured value is the pressure difference between the inlet and outlet sections of the gas mixing installation value, which is collected by the differential pressure transmitter. In the calculation, the resistance of the unit includes local resistance loss and resistance loss along the path, among which the local resistance loss is mainly caused by collision and vortex, and the resistance of the expanding area of the inlet section, the shrinking area of the outlet section, and the resistance of the spiral blade are mainly considered in the calculation process [28]. The resistance ΔP is calculated by the following formula:

$$\Delta P = \lambda \frac{L}{d}\frac{\rho u^2}{2} + \xi \frac{\rho u^2}{2}, \tag{5}$$

where λ is the resistance coefficient along the way, ξ is the local resistance coefficient, L is the length of the channel, u is the average gas velocity, and d is the equivalent diameter of the fluid channel.

According to Engineering Design Code for Utilization of Low-concentration Gas Oxidation in Coal Mines (NB/T10362-2019), the uniformity of gas mixing unit can be calculated as follows:

$$U = \left[1 - \sqrt{\frac{1}{n}\sum_{i=1}^{n}\left(\frac{c_i - \bar{c}}{\bar{c}}\right)^2}\right] \times 100\%, \tag{6}$$

where n is the number of values of methane concentration on the outlet section (uniform distribution points), c_i is the methane concentration at each point (mole fraction, the same below), and $\bar{c}$ is the average value of methane concentration at i measuring points on the section.

The Reynolds number Re is used to measure the change of internal flow of the gas mixing unit. Its physical meaning is the ratio of inertial force and viscous force of the fluid in the flow field [29], which is calculated according to the following formula:

$$\mathrm{Re} = \frac{4\rho Q_V}{\mu \pi d}, \tag{7}$$

where ρ and Q_V are, respectively, the density and volume flow of CBM at 101325 Pa and 0°C, u is the average axial flow velocity of the section, d is the diameter of section, and μ is dynamic viscosity.

The boundary conditions are set as follows:

(1) Inlet boundary conditions: the velocity inlet is adopted, and the mole fraction of methane and air at each inlet is given.

(2) Exit boundary conditions: at the exit boundary, the flow is considered to be fully developed and the exit is far away from the backflow zone.

(3) Solid wall conditions: the wall velocity meets $u_i = 0$, and the pressure meets $\partial P/\partial n = 0$.

3. Calculation Results and Discussion

The structural parameters of air mixing unit mainly include the number of spiral blades, blade pitch, and spiral length. In the following, a gas mixing unit with a flow rate of 7000 Nm^3/h is taken as an example to study the influence of changes in structural parameters on the overall flow characteristics of the unit and to analyze the general rule of changes in structural parameters on the uniformity of gas mixing and resistance loss of the unit, so as to lay a data foundation for subsequent correlation fitting analysis. Based on the previous study [30], when the author carried out numerical simulation on the air mixing unit with a flow rate of 7000 Nm^3/h, the spiral combination mode inside the unit was set as follows: the spiral direction of the small tube area was left, the spiral direction of the mixing area was right, and there was no spiral blade in the large tube area.

3.1. Number of Spiral Pieces in Mixing Zone. Figure 3 is the cloud diagram of uniformity of gas at 1 m distance from flange outlet under different blade numbers in the mixing zone. Figure 4 is the curve diagram of uniformity and resistance loss corresponding to different blade numbers. It can be seen that with the increase of the number of spiral blades, the uniformity of the unit shows an overall trend of rising first and then falling. Among them, when the number of spiral blades rises from 1 to 2, the uniformity is improved. This is because when 2 or more spiral blades are used, the flow channels in the circular tube can be reasonably and evenly distributed. When only one spiral blade is arranged, the mixed gas cannot be fully mixed after flowing around the blades. When the number of spiral blades is 2 or more, the uniformity of gas decreases with the increase of the number of spiral blades. This is because when spiral blades are arranged in a fixed diameter circular tube, with the increase of the number of spiral vanes, the port number of the gas also increases and methane and air mixed flow around inside the flow channel. Continuing only to increase the number of spiral vanes cannot improve the uniformity of gas, so this should be noted in engineering practice. In addition, the diagram also can present such a trend; namely, fluid flow resistance losses increase corresponds to the increase of the mixing zone number of spiral vanes. This is because the increase of spiral vanes makes the pipe fluid flow around the interrupted area ratio increase; the fluid increases the chance of collisions between molecules, and intuitively reflects the increase of the overall resistance of the unit.

3.2. Length of Spiral Blade in Mixing Zone. According to the air mixing characteristics in the pipe of the unit, the influence of the length of spiral blade in the mixing zone on the uniformity and pressure loss at the outlet of the unit is further investigated, as shown in Figures 5 and 6. When the blade length increases from 500 mm to 1300 mm, the uniformity of gas at the outlet of the unit decreases as a whole, while the resistance loss increases. On the basis of constant pitch of spiral blade in the mixing zone, increasing blade length will reduce the uniformity. This is because when low-concentration gas flows around the mixing zone, it only moves centrifugally to increase the kinetic energy of radial flow of the fluid itself. In this process, the gas itself does not mix effectively. Mixing begins when the gas flows out of the range of spiral blades in the mixing zone. However, since the total length of the mixing zone is constant, increasing the length of the spiral blade in the mixing zone actually reduces the effective mixing space. Therefore, with the increase of the length of spiral blades in the mixing zone, the uniformity of gas decreases. The average flow energy around the blade increases with the increase of blade length, but it is at the cost of the increase of the resistance loss inside the unit. Therefore, in practical engineering application, the length of spiral blade in mixing zone should be appropriately reduced under the condition of ensuring the uniformity of gas.

3.3. Pitch of Spiral Blade in Mixing Zone. Figure 7 shows the cloud diagram of components at the outlet of the unit corresponding to different pitch in the mixing zone, and Figure 8 shows the variation trend of the uniformity of gas at the outlet and the resistance loss with the pitch of the blade in the mixing zone. As can be seen from the figure, on the premise that the total length of the spiral blades in the mixing zone remains unchanged, increasing the pitch of the spiral blades in the mixing zone will make the uniformity of the unit decrease slowly at first and then rapidly after reaching a certain value. Conversely, resistance loss decreases rapidly and then slowly. For the 7000 Nm^3/h air mixing unit, when the blade pitch in the mixing zone changes from 400 mm to 1000 mm, the resistance loss of the unit decreases significantly, while the uniformity of gas decreases from 97% to 95%, with little change. This is because the total length of the spiral is unchanged, and the increase of the pitch means the number of spiral turns decreases, that is to say, the included angle between the spiral blade and the fluid becomes smaller, weakening the effect of gas turbulence. When the screw pitch in the mixing zone increases to 1200 mm, the mixing effect of screw pitch on the fluid is not obvious, and only the diversion effect exists. This rule is crucial for subsequent CBM mixing. In practical engineering design, it is necessary to find the inflection point of the pitch value to design the air mixing unit that meets the requirements more efficiently.

3.4. Number of Spiral Pieces in Tubule Zone. Under the condition of keeping the structural parameters of the mixing zone unchanged, the influence of the number of spiral blades in the tubule zone on the uniformity of gas and pressure loss

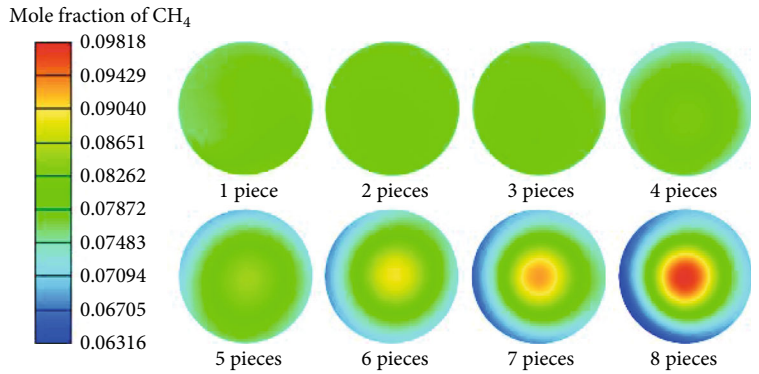

Figure 3: Effect of the number of helical blades in the mixing zone on the uniformity.

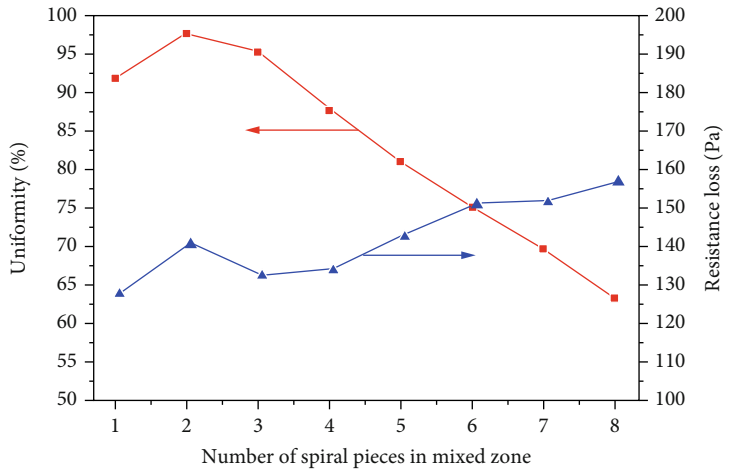

Figure 4: Effect of the number of helical blades in mixing zone on flow parameters.

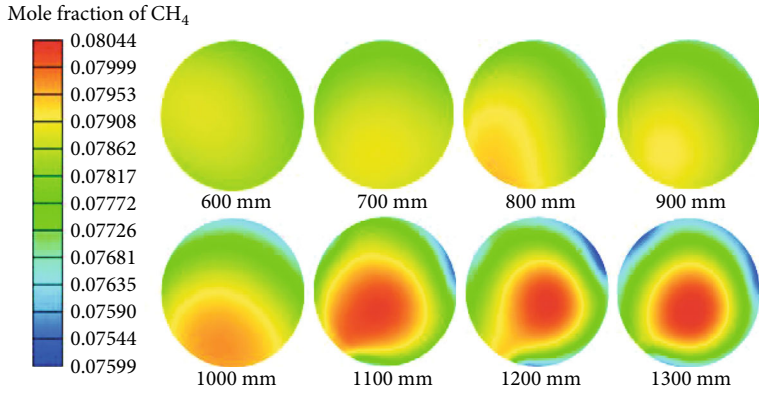

Figure 5: Influence of length of spiral blade on the uniformity in the mixing zone.

is investigated. Figure 9 shows the component cloud diagram at the outlet of the unit under different blade numbers in the small tube area. Figure 10 shows the variation trend of uniformity of gas and resistance loss at the outlet of the unit with the number of blades in the tubule zone. It can be seen that the change in the number of blades in the tubule zone has little influence on the uniformity of gas and pressure loss. For the performance of air mixing, the effect of the number of spiral blades in the tubule zone is not obvious, and the curve is flat as a whole. Therefore, in practical engineering, we can appropriately reduce the number of spiral blades in tubule zone to reduce the processing cost of the unit.

3.5. Length of Spiral Blade in Tubule Zone. By changing the length of spiral blade in the tubule zone, the influence law on the uniformity of gas and resistance loss of the unit is investigated. The related cloud diagrams and curves are

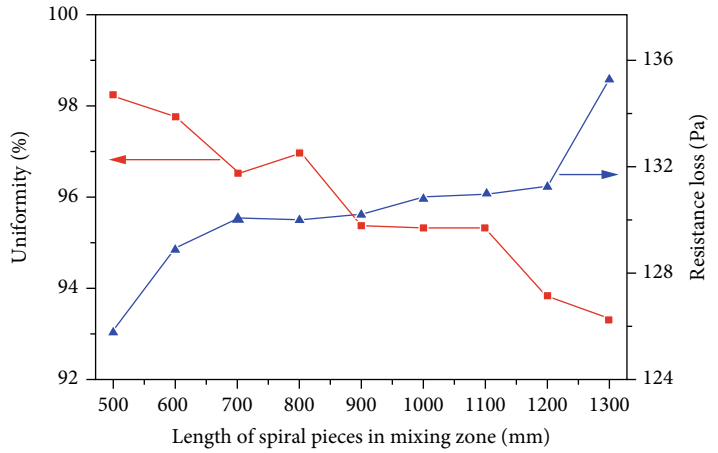

Figure 6: Influence of length of spiral blade on flow parameters in mixing zone.

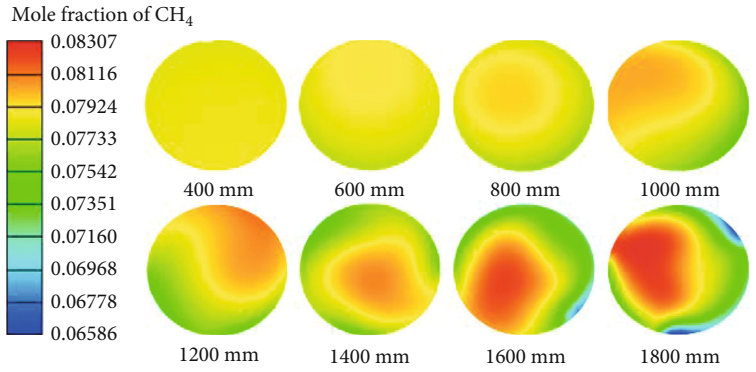

Figure 7: Influence of blade pitch on the uniformity in mixing zone.

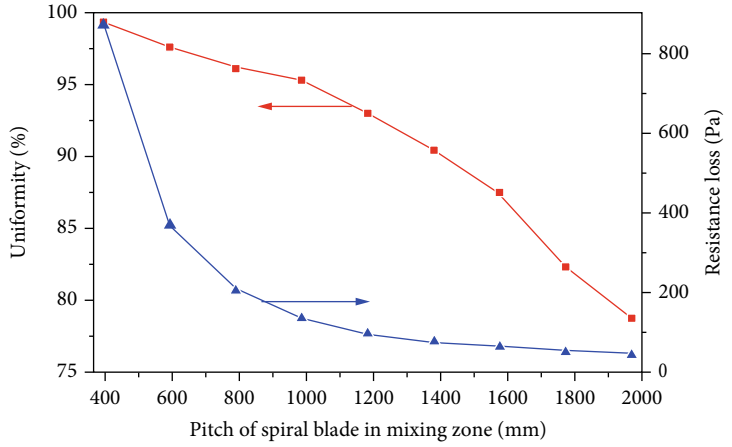

Figure 8: Influence of blade pitch on flow parameters in mixing zone.

shown in Figures 11 and 12. It can be seen from the figure that the uniformity of gas and resistance loss of the unit decrease with the increase of the length of the spiral blade of the tubule, but the variation range is small. When the length of spiral blade increases from 400 mm to 1000 mm, the resistance loss decreases only about 10 Pa. Although the first three points in Figure 12 rise, the increase is only 2 Pa, and the uniformity of gas is almost unchanged. It shows that increasing or decreasing the length of spiral blade has little effect on the performance parameters of air mixing unit. Therefore, the selection of tubular spiral blades should be balanced according to the corresponding indicators. Considering the manufacturing process and cost comprehensively, keeping the length of tubular spiral blades at a small level is a good choice.

3.6. Pitch of Spiral Blade in Tubule Zone. Figures 13 and 14 show the cloud map of methane composition at the outlet

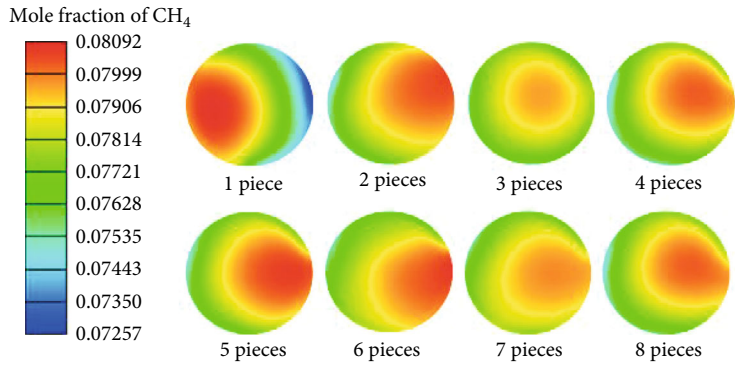

Figure 9: Influence of the number of spiral blades in the tubule zone on the uniformity.

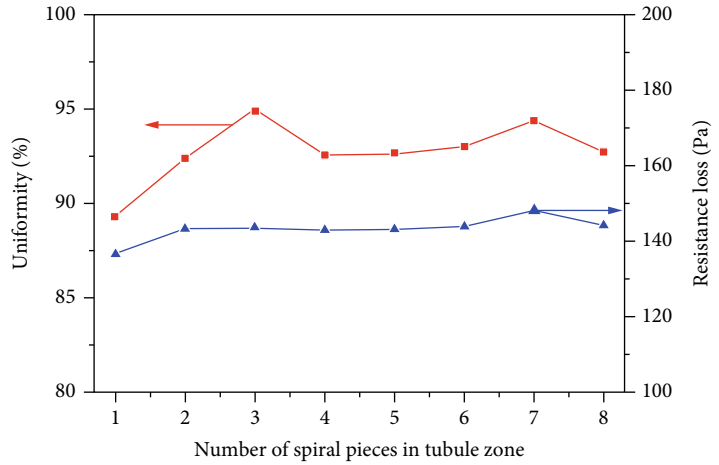

Figure 10: Influence of the number of spiral blades in the tubular zone on flow parameters.

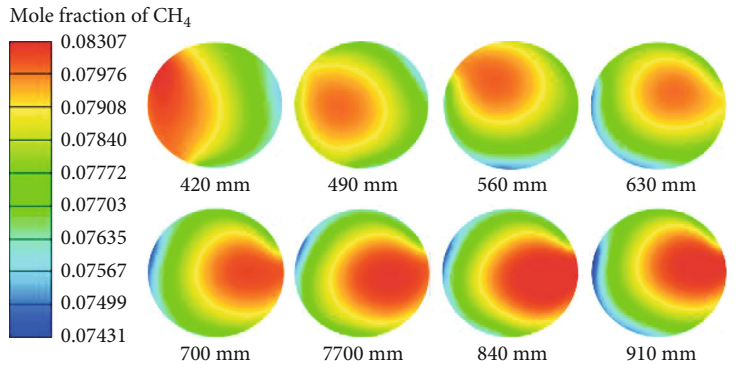

Figure 11: Influence of length of spiral blade on the uniformity of gas in tubule zone.

of the device and the change rule of corresponding curves when the pitch of spiral blade in the tubule zone is changed. Similar to those of the mixing zone screw pitch change, with the increase of the small batch screw pitch, unit flow resistance is decreased at the first, then gradually levels off; this is because when the total length of the spiral is fixed, the smaller the pitch means the greater spiral angle of blade and the gas flow. The small area of gas results in more intense collisions with spiral screw blade centrifugal effect of CBM becoming more intense. At this time, the flow rate of methane gas escaping from the small tube increases, and the collision with the fluid in the large tube becomes more intense. When the screw pitch increases to a certain value, the centrifugal effect of the screw on the fluid in the tube is weakened and only the basic diversion effect exists. Unlike the pitch change in the mixing zone, the small batch pitch increase will improve overall uniformity of mixed gas unit. This is because the pitch is small, spiral unit for a small tube of methane gas centrifugal effect is bigger, and the methane gas escape tubular will gain greater centrifugal momentum. This means that the centrifugal speed increases when leaving the small tube. As can be seen from Figure 13, when

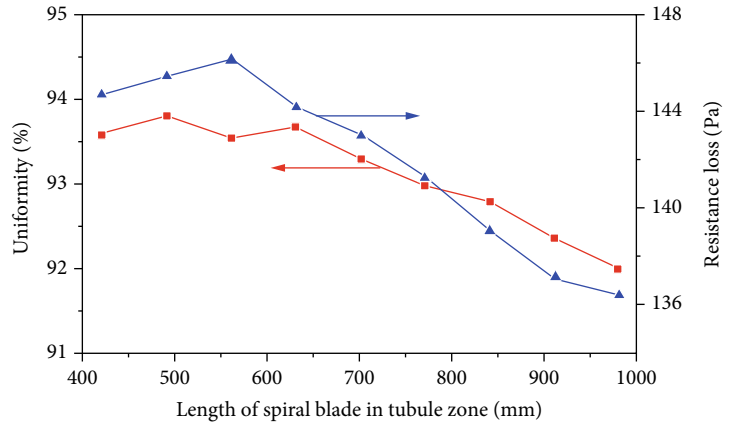

Figure 12: Influence of spiral blade length on flow parameters in tubule zone.

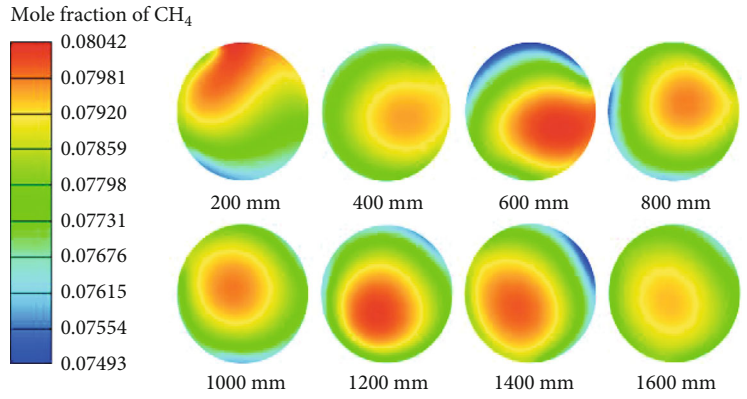

Figure 13: Influence of blade pitch in tubule zone on the uniformity of gas.

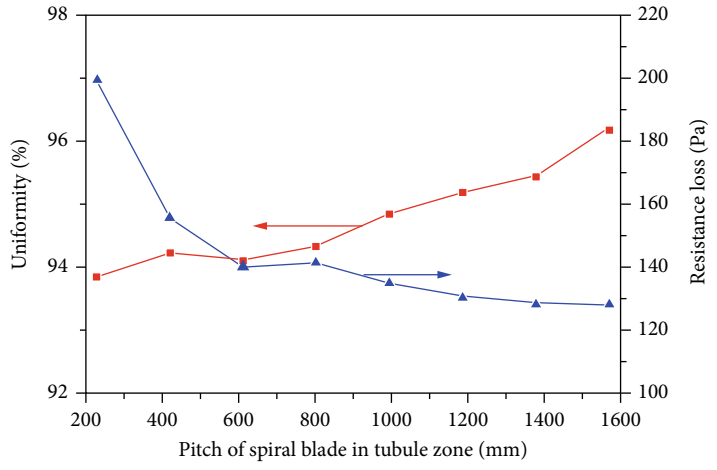

Figure 14: Influence of blade pitch on flow parameters in small tube.

methane is mixed with the large pipe fluid in the mixing zone, centrifugal action makes methane gas unable to disperse well in the mixing zone, resulting in agglomeration. At this point, the gas uniformity of the unit can be improved by appropriately increasing the pitch of the blade in the tubule zone to reduce its centrifugal effect on methane gas. Therefore, for a 7000 Nm^3/h air mixing unit, an appropriate increase in the pitch of the small tube zone can both improve the uniformity of the unit and reduce the resistance loss.

3.7. Influence of Mixed Gas Flow Rate. After the gas mixing unit is processed and installed according to the designed structure, the structure and size cannot be changed, but the flow rate of CBM is easily changed due to the influence of

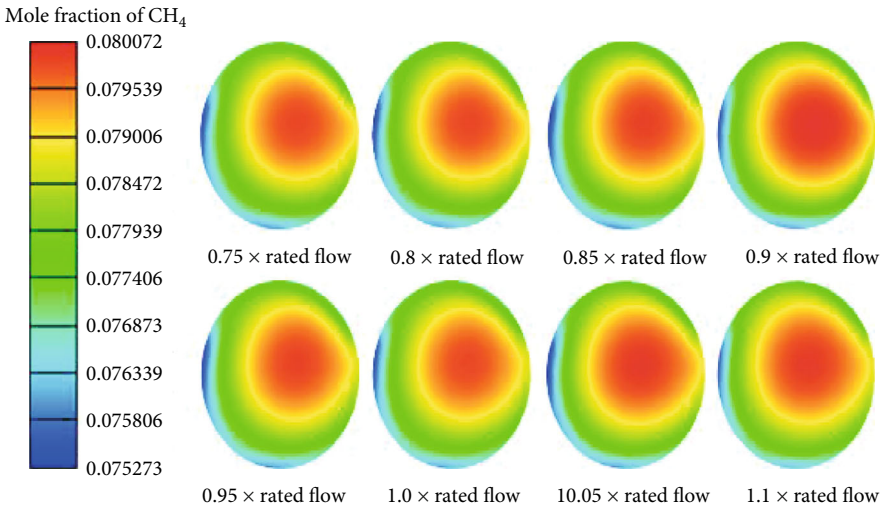

Figure 15: Influence of air mixture flow change on the uniformity of gas.

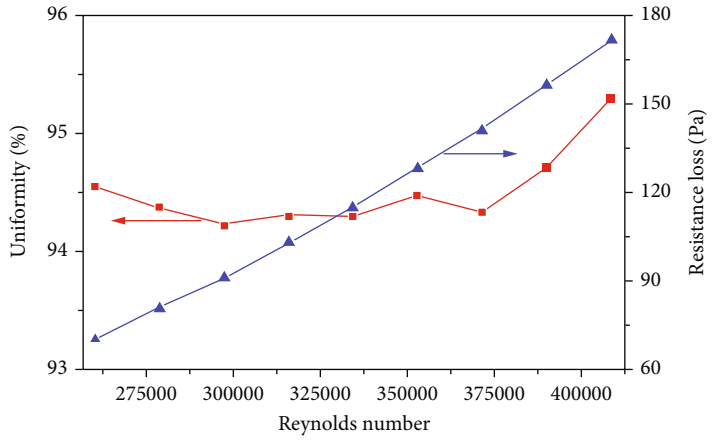

Figure 16: Influence of mixed gas flow change on flow parameters.

gas extraction conditions in the coal mine. In order to ensure the operation safety of downstream CBM utilization units, the resistance and uniformity of CBM mixing must reach the standard even if the flow rate changes.

Figures 15 and 16 show the variation trend of the mixing performance of the 7000 Nm^3/h mixing unit with the change of the operating flow rate. It can be found that with the increase of the flow rate, the resistance loss of the unit presents a linear increasing trend, and the uniformity of gas has little change within the range of the Reynolds Number of 275000-375000. However, it increases slightly after Re > 375000. According to the calculation results, the increase of uniformity can be ignored, so the designed mixing unit can still meet the requirements of uniformity of gas when the flow rate decreases. However, it is inevitable that the resistance loss increases with the increase of Reynolds number because the structure and size of the unit do not change. With the increase of gas kinetic energy, the more kinetic energy is lost due to the presence of resistance; that is, the resistance loss of the unit increases with the increase of gas flow.

4. Performance Parameter Prediction Model

The work above introduces the optimization process of the structural parameters of the 7000 Nm^3/h flow mixing unit, which is applied to the design of the mixing system of the low-concentration CBM power generation unit. The gas mixing units are analyzed and optimized with the rated flow rates of 50000 Nm^3/h (used for coal bed methane power generation) and 160000 Nm^3/h (used for coal bed methane thermal storage and oxidation) and finally obtain uniformity of gas and pressure drop of the three units under different structures and variable flow rates. The main factors affecting the gas mixing effect of each unit are analyzed, which can be used to guide the practical engineering application. Next, the influence of each influencing factor on the gas mixing effect is quantified, and the prediction of flow and gas mixing performance under each working condition is realized through mathematical correlation formula; that is, the prediction model of resistance and uniformity can be obtained.

The uniformity of gas is a dimensionless number, and the structural parameters of air mixing unit, including the

number of spiral blades, spiral length, pitch, and air mixing flow rate, all have units. Therefore, these parameters should be treated dimensionless first, so that they are only quantitatively related. The unit of spiral pitch and spiral length is the same as the unit of pipe diameter. It can be dimensionless by division, and the flow rate is generally expressed in the form of Reynolds number. The prediction model of uniformity U is as follows:

$$U = A_1 \times \left(\frac{L_m}{\mathrm{d}_m}\right)^a \times \left(\frac{\mathrm{P}_m}{d_m}\right)^b \times \left(\frac{L_s}{\mathrm{d}_s}\right)^c \times \left(\frac{P_s}{d_s}\right)^e \times \left(\frac{M_m}{M_s}\right)^f \times \mathrm{Re}^g. \tag{8}$$

The unit of resistance loss is Pa, and its prediction model is as follows:

$$\Delta P = f \times \frac{\rho u^2}{2}, \tag{9}$$

where f is friction and form resistance factor and is a dimensionless number. Considering the influence factors of friction and shape resistance factor f, the prediction model of the resistance ΔP in equation (9) is as follows:

$$\Delta \mathrm{P} = \mathrm{A}_2 \times \left(\frac{L_m}{\mathrm{d}_m}\right)^{\mathrm{h}} \times \left(\frac{\mathrm{P}_\mathrm{m}}{d_\mathrm{m}}\right)^i \times \left(\frac{L_s}{\mathrm{d}_s}\right)^j \times \left(\frac{P_s}{d_s}\right)^k \times \left(\frac{M_m}{M_s}\right)^l \times \mathrm{Re}^n \times \frac{\rho u^2}{2}. \tag{10}$$

In equations (8) and (10), Re is the Reynolds number; L is the length of the main spiral blade in the mixing zone; P is pitch; d is the inner diameter of the pipeline; M is the number of spiral blades. Subscript m is the mixing area, and s is the tubule zone. The physical meanings of L_m/d_m and L_s/d_s are the length-diameter ratio of spiral blades in the mixing zone and the tubule zone, respectively; the physical meaning of $\rho u^2/2$ is kinetic energy lost per unit volume of fluid. The task of correlation fitting is to determine the coefficients A_1, A_2, a, b, c, e, f, g, h, i, j, k, l, n, and so on.

Linear regression is performed on the calculated data to obtain the prediction mathematical models of resistance and the uniformity of gas of each air mixing device.

The following is the prediction model of 7000 Nm^3/h gas mixing plant:

$$U = 1.0768 \times \left(\frac{L_m}{\mathrm{d}_m}\right)^{-0.527} \times \left(\frac{\mathrm{P}_m}{d_m}\right)^{-0.139} \times \left(\frac{L_s}{\mathrm{d}_s}\right)^{-0.022} \times \left(\frac{P_s}{d_s}\right)^{0.033} \times \left(\frac{M_m}{M_s}\right)^{-0.241} \times \mathrm{Re}^{0.01}, \tag{11}$$

$$\Delta \mathrm{P} = 55.5845 \times \left(\frac{L_m}{\mathrm{d}_m}\right)^{0.082} \times \left(\frac{\mathrm{P}_\mathrm{m}}{d_\mathrm{m}}\right)^{-1.854} \times \left(\frac{L_s}{\mathrm{d}_s}\right)^{-0.058} \times \left(\frac{P_s}{d_s}\right)^{-0.114} \times \left(\frac{M_m}{M_s}\right)^{0.099} \times \mathrm{Re}^{0.006} \times \frac{\rho u^2}{2}. \tag{12}$$

The following is the prediction model of 50000 Nm^3/h gas mixing plant:

$$U = 0.1198 \times \left(\frac{L_m}{\mathrm{d}_m}\right)^{0.052} \times \left(\frac{\mathrm{P}_\mathrm{m}}{d_\mathrm{m}}\right)^{-0.456} \times \left(\frac{L_\mathrm{b}}{\mathrm{d}_\mathrm{b}}\right)^{-0.003} \times \left(\frac{P_\mathrm{b}}{d_\mathrm{b}}\right)^{-0.053} \times \left(\frac{M_m}{M_\mathrm{b}}\right)^{-1.177} \times \mathrm{Re}^{0.156}, \tag{13}$$

$$\Delta \mathrm{P} = 5.977 \times 10^{-5} \times \left(\frac{L_m}{\mathrm{d}_m}\right)^{0.033} \times \left(\frac{\mathrm{P}_\mathrm{m}}{d_\mathrm{m}}\right)^{-1.696} \times \left(\frac{L_b}{\mathrm{d}_b}\right)^{0.519} \times \left(\frac{P_b}{d_b}\right)^{-0.968} \times \left(\frac{M_m}{M_\mathrm{b}}\right)^{0.162} \times \mathrm{Re}^{0.94} \times \frac{\rho u^2}{2}. \tag{14}$$

The following is the prediction model of 160000 Nm^3/h gas mixing plant:

$$U = 5.3924 \times \left(\frac{L_m}{\mathrm{d}_m}\right)^{0.04} \times \left(\frac{\mathrm{P}_\mathrm{m}}{d_\mathrm{m}}\right)^{-0.104} \times \left(\frac{L_s}{\mathrm{d}_s}\right)^{-0.015} \times \left(\frac{P_s}{d_s}\right)^{0.027} \times \left(\frac{M_m}{M_s}\right)^{-1.568} \times \mathrm{Re}^{-0.156}, \tag{15}$$

$$\Delta \mathrm{P} = 2.0198 \times \left(\frac{L_m}{\mathrm{d}_m}\right)^{0.323} \times \left(\frac{\mathrm{P}_\mathrm{m}}{d_\mathrm{m}}\right)^{-1.859} \times \left(\frac{L_s}{\mathrm{d}_s}\right)^{0.013} \times \left(\frac{P_s}{d_s}\right)^{-0.069} \times \left(\frac{M_m}{M_s}\right)^{0.096} \times \mathrm{Re}^{0.041} \times \frac{\rho u^2}{2}. \tag{16}$$

By comparing the numerical simulation and prediction model of three sets of gas mixing units, the prediction model corresponds well with the simulation value on the whole (Figure 17 shows the comparison between the simulated calculated value and the associated predicted value of some structural parameters of the 7000 Nm^3/h unit, and the comparison diagrams of 50000 Nm^3/h and 160000 Nm^3/h are omitted here). Both the uniformity of gas and the resistance loss are basically consistent in the overall trend, and the maximum relative error between most of the simulated values and the calculated values of the prediction model is less than 10%. Local parts cannot fit well; the main reason is as follows: first of all, because there are as many as seven variables in each formula and each independent variable influences the uniformity of gas and resistance loss differently, in the process of formula fitting, in order to ensure the main influencing factors for gas mixed results, the influence of secondary parameters effect is weakened. Secondly, it can be seen from Figure 17 that the results of simulation operation fluctuate in some places. The mathematical model expressed in equations (11)–(16) has weakened the influence of these fluctuation points. Therefore, near these points, the relative error between the simulation value and the calculated value of the prediction model is large, which belongs to the normal phenomenon of simulation operation.

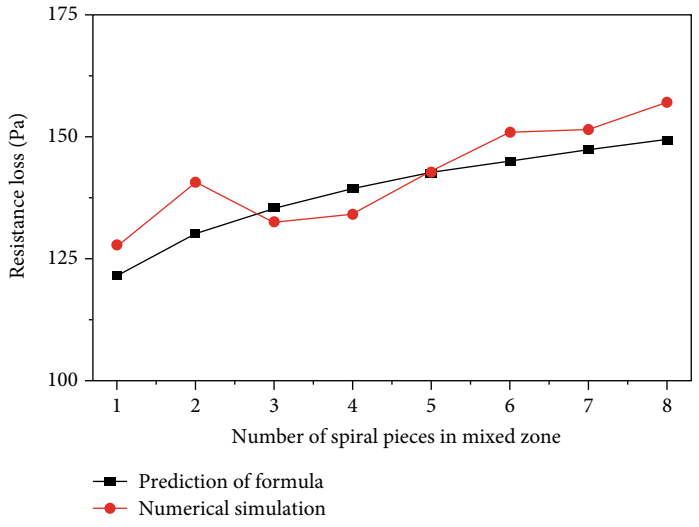

(a) Number of screws in mixing zone-resistance loss

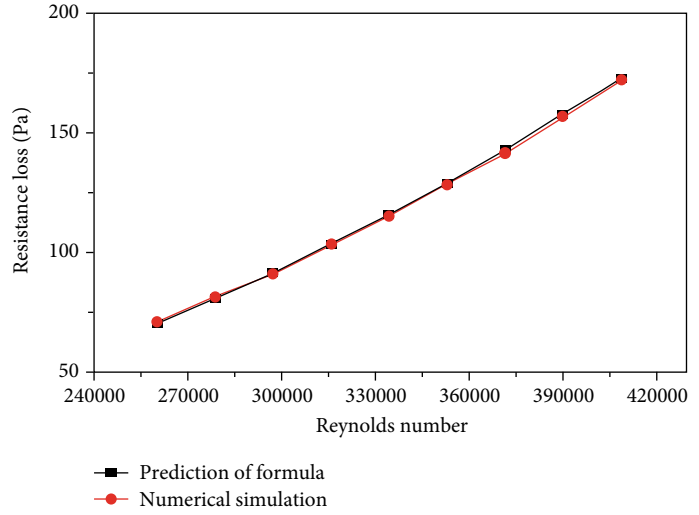

(b) Reynolds number-resistance loss

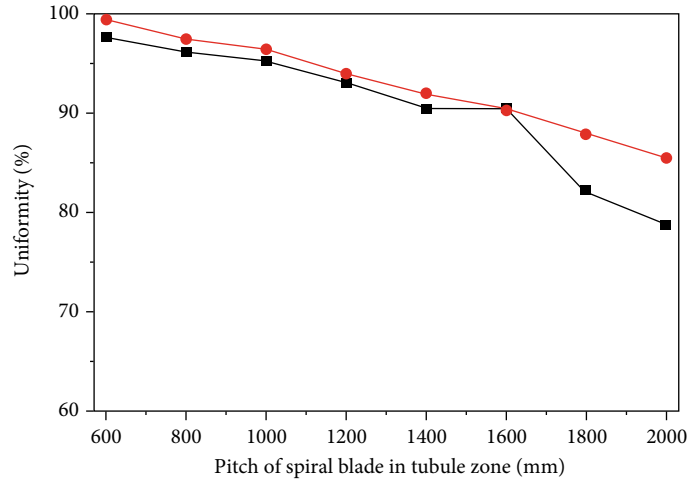

(c) Tubule pitch-uniformity of gas

Figure 17: Continued.

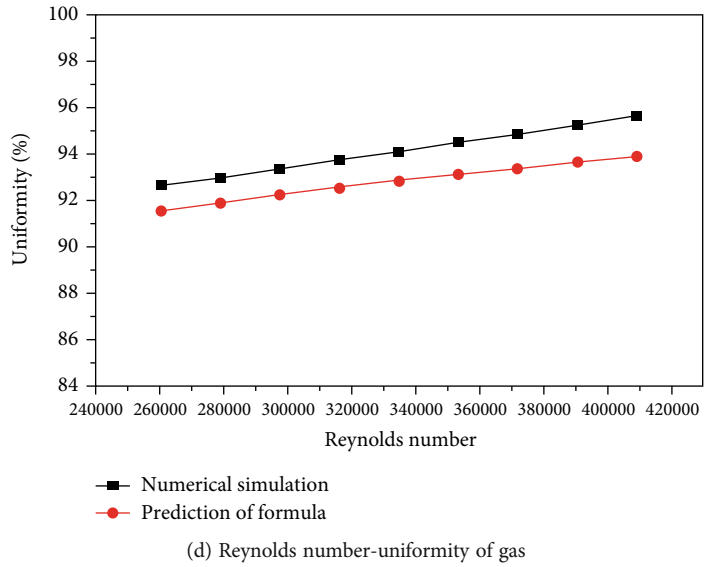

(d) Reynolds number-uniformity of gas

Figure 17: Comparison between simulation and correlation predicted value of gas mixing unit (7000 Nm^3/h).

Table 1: Structural parameters of gas mixing unit during processing.

Flow (Nm^3/h)	Tubule zone			Mixing zone		
	Number of slices	Pitch (mm)	Length (mm)	Number of slices	Pitch (mm)	Length (mm)
7000	4	1400	700	3	1000	500
50000		Not set		3	2000	1600
160000	4	1400	700	2	2636	1845

5. Comparison of Experimental Results

In order to evaluate the accuracy of the above calculation results, it is necessary to carry out experimental verification. According to the numerical simulation results, three sets of CBM mixing units are processed according to the structural parameters shown in Table 1, with rated flows of 7000 Nm^3/h (used for CBM power generation), 50000 Nm^3/h (used for CBM power generation), and 160000 Nm^3/h (used for CBM heat storage and oxidation), respectively. In the gas mixing device with a flow rate of 50000 Nm^3/h, the flow rate and concentration in the small pipe area are 45000 Nm^3/h and 0% (air), respectively, and the flow rate and concentration in the large pipe area are 5000 Nm^3/h and 10%, respectively. The average concentration of methane after mixing is 1%. In the gas mixing device with a flow rate of 160000 Nm^3/h, the flow rate and concentration of small pipe are 150400 Nm^3/h and 0% (air), respectively; and the flow rate and concentration of large pipe are 9600 Nm^3/h and 10%, respectively. The average concentration of methane after mixing is 0.6%.

After processing, they are installed on the inlet pipe of the front end of each service CBM utilization unit. Differential pressure transmitters are arranged at the inlet and outlet of the mixing unit to measure the resistance loss of the unit. In the test system, uniformity is calculated from methane concentration values at different radial positions on the outlet section. As shown in Figure 18, the methane concentration sensor is arranged on the same section of the mixer outlet, and the sampling pipe is also distributed in the center line in the cross section. The amount of methane concentration sensors can be set according to the size of diameter of

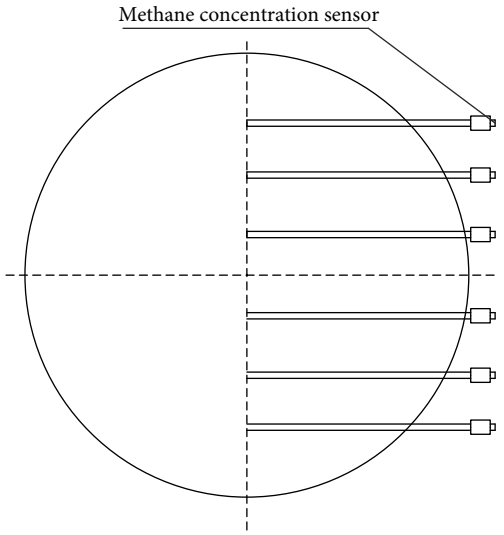

Figure 18: Layout of gas uniformity measuring points of gas mixing unit.

Table 2: Comparison between calculation and measured results of gas mixing unit.

Flow (Nm^3/h)	Resistance ΔP (Pa)		Uniformity U	
	Calculated value	Measured value	Calculated value	Measured value
7000	81	94	97.80%	99.20%
50000	286	325	90.76%	98.80%
160000	498	485	91.46%	97.20%

Figure 19: Arrangement of spiral blades in the experimental unit.

mixed instruments and limitations of cost. In this experiment, 6 sets of methane concentration sensors are arranged in each mixing unit. After measuring methane concentration at each point at the same time, uniformity can be calculated according to the equation (6).

After the CBM utilization unit ran stably, the resistance and uniformity of three units are tested at a rated flow rate, and compared with the calculated values (as shown in Table 2). A certain error is found between the calculated values and the measured values.

The roughness of the wall surface and the processing technology of the spiral blade could be the key factors causing resistance error in the experimental unit. Increasing the wall roughness can improve the pressure drop of the unit. Ordinary carbon steel is used in the processing of the air mixing unit, and the wall roughness is set at 0.06 during calculation, which may be different from the actual value of the unit (as shown in Figure 19). In terms of processing technology, the blade of the unit is not formed by mold integration, but by a manual bending method. Therefore, in the process of manufacturing and assembly, the change of blade cross section angle and the reservation of necessary clearance in the process of manufacturing will lead to the increase of measuring pressure loss of the unit, but these factors cannot be fully reflected in the numerical simulation.

CBM utilization unit requires that the resistance of mixing unit is not more than 500 Pa and the uniformity of gas is not less than 90%. If the machine parameters are not reasonable, it is difficult to meet the above two performance requirements. Although there are errors between the calculation results and the experimental measured values, the structural parameters of the unit are optimized to meet the requirements of the CBM utilization unit for the resistance and uniformity of the gas mixing unit. Through numerical simulation, technical measures can be provided to reduce the resistance of the unit, improve the uniformity of CBM mixing with different concentrations, and provide safety guarantee measures for the downstream CBM utilization unit.

6. Conclusion

(1) The concentration of low-concentration CBM extracted from underground coal mine changes frequently, which brings risks to the safe operation of oxygenated CBM utilization unit. The gas mixing unit can provide feed gas with stable methane concentration to ensure the safety and stability of the operation of the oxygenated CBM utilization unit. In the utilization of CBM, the resistance of the gas mixing unit shall not be greater than 500 Pa and the uniformity shall not be less than 90%.

(2) In this paper, the construction method of three-dimensional calculation model of low-concentration CBM gas mixing unit is studied, and the three-dimensional calculation model is constructed. The experimental unit is processed according to the structural parameters optimized by the model, and the calculation results are verified experimentally. Due to the defects in the processing technology of spiral blade structure, there are errors between simulation calculation and experimental measurement data. However, numerical simulation can provide technical measures for reducing the resistance of the unit and improving the uniformity of CBM mixing with different concentrations

(3) The overall spiral structure parameters are optimized for three sets of units with different flow rates, and the effects of different structure parameters on the mixing effect of the unit are studied. On this basis, the optimal structural parameters are optimized for three sets of units with different flow rates. When the flow rate is 7000 Nm^3/h, 50000 Nm^3/h, and 160000 Nm^3/h, the number of blades in the mixing zone is 3, 3, and 2, and the pitch is 1000 mm, 2000 mm, and 2636 mm, respectively. Blade length is 500 mm, 1600 mm, and 1845 mm; for the small tube area, the mixing unit of 50000 Nm^3/h is not equipped with blades. The number of blades of the other two units is 4, the pitch is 1400 mm, and the blade length is 700 mm

(4) The dimensionless mathematical correlations are established for the uniformity of gas and flow resistance of the three sets of units, respectively, and the maximum error is controlled within 10% with the simulation results, which provide guidance for the design of other scale gas mixing units

Data Availability

The data that support the findings of this study are available from the corresponding author.

Conflicts of Interest

The author declares that they have no conflicts of interest.

Acknowledgments

This work was supported by Chongqing Talent Plan Innovation and Entrepreneurship Leading Talent Project (CQYC201903009) and China National Science and Technology Major Project (2016ZX05045-006).

References

[1] H. Jie, Z. Changchun, H. Zhaohui et al., "Log evaluation of a coalbed methane (CBM) reservoir: a case study in the southern Qinshui basin, China," *Journal of Geophysics and Engineering*, vol. 11, article 015009, 2014.

[2] L. Ma, B. Liu, Y. Cui, and Y. Shi, "Variations and drivers of methane fluxes from double-cropping paddy fields in Southern China at diurnal, seasonal and inter-seasonal timescales," *Water*, vol. 13, no. 16, p. 2171, 2021.

[3] D. W. Kweku, O. Bismark, A. Maxwell et al., "Greenhouse effect: greenhouse gases and their impact on global warming," *Journal of Scientific research and reports*, vol. 17, no. 6, pp. 1–9, 2018.

[4] P. Ge, M. Chen, Y. Cui, and D. Nie, "The research progress of the influence of agricultural activities on atmospheric environment in recent ten years: a review," *Atmosphere*, vol. 12, no. 5, p. 635, 2021.

[5] S. Tao, S. Chen, and Z. Pan, "Current status, challenges, and policy suggestions for coalbed methane industry development in China: a review," *Energy Science & Engineering*, vol. 7, no. 4, pp. 1059–1074, 2019.

[6] S. Tao, Z. Pan, S. Tang, and S. Chen, "Current status and geological conditions for the applicability of CBM drilling technologies in China: a review," *International Journal of Coal Geology*, vol. 202, pp. 95–108, 2019.

[7] G. Kang, T. Kang, J. Guo et al., "Effect of electric potential gradient on methane adsorption and desorption behaviors in lean coal by electrochemical modification: implications for coalbed methane development of Dongqu Mining, China," *ACS omega*, vol. 5, no. 37, pp. 24073–24080, 2020.

[8] Y. Li, S. Pan, S. Ning, L. Shao, Z. Jing, and Z. Wang, "Coal measure metallogeny: metallogenic system and implication for resource and environment," *Science China Earth Sciences*, vol. 65, no. 7, pp. 1211–1228, 2022.

[9] Y. Li, C. Zhang, D. Tang et al., "Coal pore size distributions controlled by the coalification process: an experimental study of coals from the Junggar, Ordos and Qinshui basins in China," *Fuel*, vol. 206, pp. 352–363, 2017.

[10] A. Zhu, Q. Wang, D. Liu, and Y. Zhao, "Analysis of the characteristics of CH4 emissions in China's coal mining industry and research on emission reduction measures," *International Journal of Environmental Research and Public Health*, vol. 19, no. 12, p. 7408, 2022.

[11] J. Zhang, H. Liu, F. Zhou, X. Li, K. Wei, and J. Song, "Enrichment of oxygen-containing low-concentration coalbed methane with CMS-3KT as the adsorbent," *ACS Omega*, vol. 6, no. 10, pp. 6914–6923, 2021.

[12] Y. Li, Z. Wang, S. Tang, and D. Elsworth, "Re-evaluating adsorbed and free methane content in coal and its ad- and desorption processes analysis," *Chemical Engineering Journal*, vol. 428, article 131946, 2022.

[13] Y. Li, Y. Wang, J. Wang, and Z. Pan, "Variation in permeability during CO_2-CH_4 displacement in coal seams: part 1 - experimental insights," *Fuel*, vol. 263, article 116666, 2020.

[14] H. Pu, L. Zhang, X. Dong, T. Jing, and X. Junce, "Simulation of the extraction efficiency of coalbed methane under water injection: a gas-liquid-solid coupling model," *Geofluids*, vol. 3, 14 pages, 2020.

[15] Y. Zhou, X. Ji, and J. Tang, "Prospect analysis of high temperature air combustion technology for low calorific value coalbed methane in Liupanshui area of Guizhou province," *IOP Conference Series: Earth and Environmental Science*, vol. 431, no. 1, pp. 012057–012057, 2020.

[16] Y. Chen and M. Wang, "China's contribution and the Chinese approach to tackling global climate change," *Chinese Journal of Urban and Environmental Studies*, vol. 9, no. 3, p. 2150018, 2021.

[17] Y. K. Dwivedi, L. Hughes, A. K. Kar et al., "Climate change and COP26: are digital technologies and information management part of the problem or the solution? An editorial reflection and call to action," *International Journal of Information Management*, vol. 63, article 102456, 2022.

[18] H. Wen, X. Cheng, J. Chen et al., "Micro-pilot test for optimized pre-extraction boreholes and enhanced coalbed methane recovery by injection of liquid carbon dioxide in the Sangshuping coal mine," *Process Safety and Environmental Protection*, vol. 136, pp. 39–48, 2020.

[19] K. Wang, J. Zhang, B. Cai, and S. Yu, "Emission factors of fugitive methane from underground coal mines in China: estimation and uncertainty," *Applied Energy*, vol. 250, pp. 273–282, 2019.

[20] L. Xiao and J. Chen, "Experimental study on heat transfer caused by feed gas concentration fluctuation in low concentration CBM utilization unit," *Heat and Mass Transfer*, vol. 58, no. 2, pp. 355–363, 2022.

[21] P.-F. Gao and X.-L. Gou, "Experimental research on the thermal oxidation of ventilation air methane in a thermal reverse flow reactor," *ACS Omega*, vol. 4, no. 12, pp. 14886–14894, 2019.

[22] S. Ren, L. Huang, L. Zhang et al., "Explosion limit test of high pressure and high temperature methane air mixture," *Journal of China University of Petroleum (NATURAL SCIENCE EDITION)*, vol. 43, pp. 98–103, 2019.

[23] Q. Bo, "Design and research of low concentration gas power generation system in t coal mine," *Mechanical management development*, vol. 30, pp. 16–18, 2015.

[24] L. Wang, Z. Li, G. Mao, Y. Zhang, and F. P. Lai, "Effect of nanoparticle adsorption on the pore structure of a coalbed methane reservoir: a laboratory experimental study," *ACS Omega*, vol. 7, no. 7, pp. 6261–6270, 2022.

[25] J. Chen, G. Wen, S. Yan, X. Lan, and L. Xiao, "Oxidation and characterization of low-concentration gas in a high-temperature reactor," *Processes*, vol. 8, no. 4, p. 481, 2020.

[26] Y. Li, D. Guo, and X. Li, "The effect of startup modes on a vacuum cam pump," *Vacuum*, vol. 166, pp. 170–177, 2019.

[27] Y. Yuan, C. Li, and Q. Yang, "Mixed finite element-second order upwind fractional step difference scheme of Darcy–Forchheimer miscible displacement and its numerical

analysis," *Journal of Scientific Computing*, vol. 86, no. 2, pp. 1–19, 2021.

[28] S. Zhenglu, W. Yongtang, L. Hong, D. Aihua, S. Yunxin, and Y. Bin, "Design and uniformity analysis of fully premixed natural gas burner venturi mixer," *IOP Conference Series: Materials Science and Engineering*, vol. 721, article 012009, 2020.

[29] G. Gecim and E. Erkoc, "Hydrodynamics of similar gases in vortex mixers: effect of physical properties on the onset of instability," *Industrial & Engineering Chemistry Research*, vol. 61, no. 2, pp. 1192–1206, 2022.

[30] L. Xiao, "Numerical simulation and experimental analysis of dynamic continuous operation of low-concentration coalbed-methane-mixing device," *Processes*, vol. 10, no. 7, p. 1265, 2022.